Alexandria Engineering Journal (2016) 55, 2299–2308

HOSTED BY

Alexandria University

Alexandria Engineering Journal

www.elsevier.com/locate/aej
www.sciencedirect.com

ORIGINAL ARTICLE

Two parameters Lie group analysis and numerical solution of unsteady free convective flow of non-Newtonian fluid

M.J. Uddin [a,*], M.M. Rashidi [b,c], Hamed H. Alsulami [d], S. Abbasbandy [e], N. Freidoonimeh [b]

[a] Department of Mathematics, American International University-Bangladesh, Banani, Dhaka, 1213, Bangladesh
[b] Shanghai Key Lab of Vehicle Aerodynamics and Vehicle Thermal Management Systems, Tongji University, 4800 Cao An Rd., Jiading, Shanghai 201804, China
[c] ENN-Tongji Clean Energy Institute of Advanced Studies, Tongji University, China
[d] Department of Mathematics, Faculty of Science, King Abdulaziz University, Jeddah 21589, Saudi Arabia
[e] Department of Mathematics, Science and Research Branch, Islamic Azad University, Tehran, Iran

Received 15 February 2016; revised 19 April 2016; accepted 11 May 2016
Available online 31 May 2016

KEYWORDS

Non-Newtonian fluid;
Numerical solution;
Runge–Kutta–Fehlberg method;
Lie group

Abstract The two-dimensional unsteady laminar free convective heat and mass transfer fluid flow of a non-Newtonian fluid adjacent to a vertical plate has been analyzed numerically. The two parameters Lie group transformation method that transforms the three independent variables into a single variable is used to transform the continuity, the momentum, the energy and the concentration equations into a set of coupled similarity equations. The transformed equations have been solved by the Runge–Kutta–Fehlberg fourth-fifth order numerical method with shooting technique. Numerical calculations were carried out for the various parameters entering into the problem. The dimensionless velocity, temperature and concentration profiles were shown graphically and the skin friction, heat and mass transfer rates were given in tables. It is found that friction factor and heat transfer (mass transfer rate) for methanol are higher (lower) than those of hydrogen and water vapor. Friction factor decreases while heat and mass transfer rate increase as the Prandtl number increases. Friction (heat and mass transfer rate) factor of Newtonian fluid is higher (lower) than the dilatant fluid.

1. Introduction

Studies of non-Newtonian fluids flow have received much attention and importance than Newtonian fluids, due to their various technological and industrial applications. If there is a

* Corresponding author. Tel.: +880 60104625506.
E-mail addresses: jashim_74@yahoo.com (M.J. Uddin), mm_rashidi@tongji.edu.cn (M.M. Rashidi).
Peer review under responsibility of Faculty of Engineering, Alexandria University.

http://dx.doi.org/10.1016/j.aej.2016.05.009

Nomenclature

A	constant
B	constant
$\overline{C}$	concentration
C_f	skin friction factor
D	mass diffusivity
f	dimensionless velocity functions
g	acceleration due to gravity
Gr	Grashof number
K	consistency coefficient
L	reference length
N	buoyancy ratio
n	exponents identifying non-Newtonian behavior
Nb	Brownian motion
Nu	Nusselt number
Pr	Prandtl number
Ra	Rayleigh number
Re	Reynolds number
Ri	Richardson number
Sc	Schmidt number
Sh	Sherwood number
$\overline{T}$	temperature
$\bar{t}$	time
$\bar{u}$	velocity in the $\bar{x}$-direction
U	reference velocity
$\bar{v}$	velocity in the $\bar{y}$-direction
$\bar{x}$	distance along the surface
$\bar{y}$	distance normal to the surface

Greek letters

α	molecular diffusivity
α_i	constant
β_i	constant
β_C	coefficient of mass expansion
β_T	coefficient of thermal expansion
ϕ	dimensionless concentration
η	similarity variable
θ	dimensionless temperature
ρ	density of the ambient fluid
ψ	stream function

Subscript, Superscript

∞	conditions far away from the surface
$'$	differentiation with respect to η
w	wall

nonlinear relationship between stress and the rate of strain, a fluid could be said to be non-Newtonian, such that the viscosity is a function of variables such as temperature and density. Examples of non-Newtonian fluids are mud, paste, personal care products, ice cream, paints, oils, cheese, asphalt. Many biological fluids with higher molecular weight components are also non-Newtonian in nature. Non-Newtonian fluids have many applications in industries such as coal slurries, polymers solution or melts, paints, greases, drilling mud and hydrocarbon oils [1–6]. For describing the properties of non-Newtonian fluids, there are many models. These models or constitutive equations, however cannot describe all the behaviors of these non-Newtonian fluids, for example, normal stress differences, shear thinning or shear thickening, stress relaxation, elastic effects and memory effects. A rigorous study of the boundary layer flow and heat transfer of different non-Newtonian fluids past a stretching sheet was required due to its immense industrial applications. Many authors have embarked on the study of non-Newtonian flow for various reasons and using different methods of solution. Advancement in the study of various non-Newtonian fluids has been made even by many investigators (see Refs. [7–12]). Recently, Hayat et al. [13] studied third grade fluid over an unsteady permeable stretching sheet using HM. Shafiq et al. [14] studied magnetohydrodynamic axisymmetric flow of a third grade fluid between two porous disks. It is to certify that there are several limitations for the applied model for the analysis based on the non-Newtonian fluids; however, these models are still useful tools and employed in different analysis in order to formulate and study the roles of non-Newtonian fluids in different conditions and geometries (See these related papers [15–19]).

The steady viscous incompressible flow of a non-Newtonian power-law fluid on a two-dimensional body in the presence of a magnetic field was studied by Sarpkaya [20] and Djukic [21,22]. Andersson et al. [23] have considered the steady MHD flow of a power-law fluid over a linearly stretching surface. The flow and heat transfer of a power-law fluid over a uniform moving surface with a constant parallel free stream in the presence of a magnetic field have been studied by Kumari and Nath [24]. Liao [25] has obtained an analytical solution of the MHD of a non-Newtonian power-law fluid over a linearly stretching surface. Among the most popular useful models for non-Newtonian fluids is the power-law or Ostwald-de Waele model [26]. The steady flow and heat transfer of a viscous incompressible power-law fluid over a rotating infinite disk have been investigated by Ming et al. [27]. This model is a simple nonlinear equation of state for inelastic fluids which includes linear Newtonian fluids as a special case. The power-law model provides an adequate representation of many non-Newtonian fluids over the most important range of shear rates. This, together with its apparent simplicity, has made it a very attractive model in both analytical research and numerical research. Pascal [28] presented similarity solutions to some unsteady flows of non-Newtonian fluids of power law behavior. Pascal and Pascal [29] studied the nonlinear effects on some unsteady non-Darcian flows through porous media. Unsteady forced convection heat transfer on a flat plate embedded in the fluid-saturated porous medium with inertia effect and thermal dispersion is investigated by Wen and Hsiao [30]. Israel-Cookey et al. [31] discussed the influence of viscous dissipation and radiation on unsteady MHD free-convection flow past an infinite heated vertical plate in a porous medium with time-dependent suction. Recently, Chiem and Zhao [32]

studied the problem of numerical study of steady/unsteady flow and heat transfer in porous media using a characteristic-based matrix-free implicit FV method on unstructured grids.

Some of the most related papers in this area are as follows: Lee et al. [33] presented a theoretical analysis that brings steady, laminar free convection from a vertical flat plate immersed in a power-law stratified fluid within the framework of classical boundary-layer theory. Laminar two-dimensional unsteady mixed-convection boundary-layer flow of a viscous incompressible fluid past a sharp wedge has been studied by Hossain et al. [34]. Ece and Buyuk [35] investigate steady, laminar free-convection boundary-layer flow of a power-law fluid over a vertical heated plate under mixed thermal boundary conditions. A numerical examination of the problem of unsteady free convection with heat and mass transfer from an isothermal vertical flat plate to a non-Newtonian fluid saturated porous medium has been done by Elgazery [36]. Merkin and Pop [37] considered the similarity equations for mixed convection boundary-layer flow over a vertical semi-infinite at plate in which the free stream velocity is uniform and the wall temperature is inversely proportional to the distance along the plate. Rashidi et al. [38] presented new analytical method for the study of natural convection flow of a non-Newtonian. Similar problems have been investigated by others [39,40]. Most of foregoing researchers investigate the steady free convection to power-law fluids. However, all the process at early time are time dependent phenomena. To better design and control them, knowing this dependency is important. Some new published papers regarding convective flow can be found in [50–54].

In this paper, the unsteady laminar incompressible free convective heat and mass transfer flow of a non-Newtonian fluid adjacent to a vertical plate is considered. The coupled governing equations are transformed into ordinary differential equations using tow parameter Lie group of transformations. The fourth fifth order Runge–Kutta–Fehlberg and shooting method are applied to solve the ODEs.

2. Mathematical model

Consider unsteady two dimensional laminar free convective heat and mass transfer flow of a non-Newtonian fluid adjacent to a vertical plate. The physical scenario is shown in Fig. 1. The field variables within boundary-layers are the velocity components $\bar{u}$ and $\bar{v}$ along (the $\bar{x}$-axis) and normal to the plate (the $\bar{y}$-axis), the temperature $\overline{T}$ and the concentration $\overline{C}$. By using the standard power-law viscosity model and the Boussinesq assumption, the coupled boundary-layer equations describing mass, momentum and energy conservation are

$$\frac{\partial \bar{u}}{\partial \bar{x}}+\frac{\partial \bar{v}}{\partial \bar{y}}=0, \tag{1}$$

$$\frac{\partial \bar{u}}{\partial \bar{t}}+\bar{u}\frac{\partial \bar{u}}{\partial \bar{x}}+\bar{v}\frac{\partial \bar{u}}{\partial \bar{y}}=\frac{K}{\rho}\frac{\partial}{\partial \bar{y}}\left[\left|\frac{\partial \bar{u}}{\partial \bar{y}}\right|^{n-1}\frac{\partial \bar{u}}{\partial \bar{y}}\right]+g\beta_T(T-T_\infty)+g\beta_C(C-C_\infty), \tag{2}$$

$$\frac{\partial \overline{T}}{\partial \bar{t}}+\bar{u}\frac{\partial \overline{T}}{\partial \bar{x}}+\bar{v}\frac{\partial \overline{T}}{\partial \bar{y}}=\alpha\frac{\partial}{\partial \bar{y}}\left[\left|\frac{\partial \bar{u}}{\partial \bar{y}}\right|^{n-1}\frac{\partial \overline{T}}{\partial \bar{y}}\right], \tag{3}$$

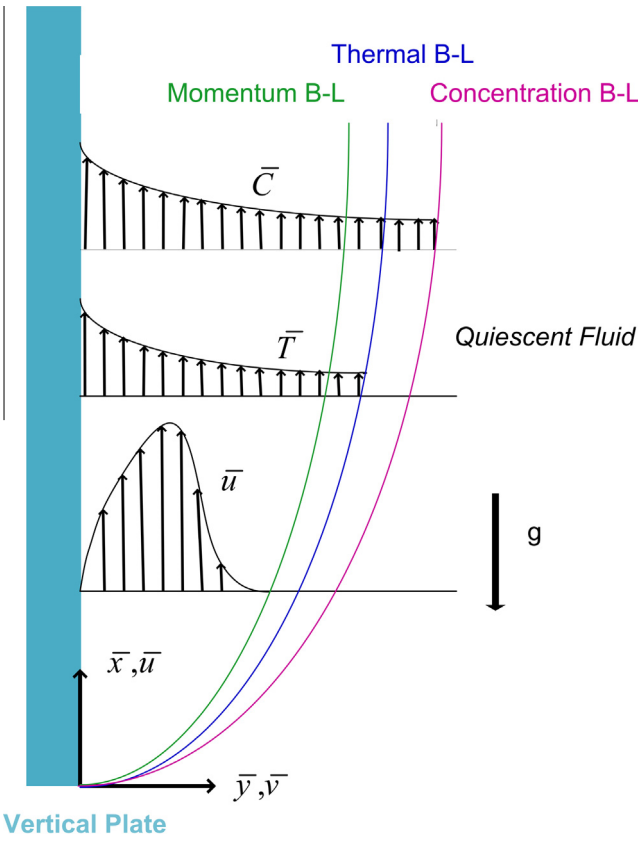

Figure 1 The schematic of the problem and coordinate system.

$$\frac{\partial \overline{C}}{\partial \bar{t}}+\bar{u}\frac{\partial \overline{C}}{\partial \bar{x}}+\bar{v}\frac{\partial \overline{C}}{\partial \bar{y}}=D\frac{\partial^2 \overline{C}}{\partial \bar{y}^2}. \tag{4}$$

The boundary conditions are

$$\begin{aligned}&\bar{v}(\bar{x},0,\bar{t})=\bar{u}(\bar{x},0,\bar{t})=0,\ \ T(\bar{x},0,\bar{t})=\overline{T}_w+\left(\overline{T}_w-\overline{T}_\infty\right)\tfrac{\bar{x}}{\bar{t}^2},\\ &\overline{C}(\bar{x},0,\bar{t})=\overline{C}_w+\left(\overline{C}_w-\overline{C}_\infty\right)\tfrac{\bar{x}}{\bar{t}^2},\bar{u}(\bar{x},\infty,\bar{t})\to 0,\\ &\overline{T}(\bar{x},\infty,\bar{t})\to\overline{T}_\infty,\ \ \overline{C}(\bar{x},\infty,\bar{t})\to\overline{C}_\infty.\end{aligned} \tag{5}$$

Here g is the acceleration due to gravity, α is the molecular diffusivity, D is the mass diffusivity, K is the consistency coefficient, ρ is the density of the ambient fluid, β_T is the coefficient of thermal expansion, β_C is the coefficient of mass expansion. The suffixes w,∞ indicate the conditions at the plate and in the ambient medium respectively. We non-dimensionalized the governing equations using the following variables:

$$\begin{aligned}&x=\frac{\bar{x}}{L},\ \ y=\frac{\bar{y}}{L}Re_n^{\frac{1}{(n+1)}},\ \ u=\frac{\bar{u}}{U},\ \ v=\frac{\bar{v}}{U}Re_n^{\frac{1}{(n+1)}},\\ &T=\frac{\overline{T}-\overline{T}_\infty}{\overline{T}_w-\overline{T}_\infty},\ \ C=\frac{\overline{C}-\overline{C}_w}{\overline{C}_\infty-\overline{C}_w},\ \ t=\frac{\bar{t}U}{L},\end{aligned} \tag{6}$$

where $U=\sqrt{g\beta_T(T_w-T_\infty)L}$ is the reference velocity, L is the reference length, and $Re_n=\rho U^{2-n}L^n/K$ is the generalized Reynolds number, $Re=\rho UL/\mu$ is the Reynolds number. Also, introducing stream function $\psi(x,y,t)$ defined as $u=\frac{\partial\psi}{\partial y}$, $v=-\frac{\partial\psi}{\partial x}$, which automatically satisfies the mass conservation Eq. (1) and Eqs. (2)–(4) becomes

$$\frac{\partial^2\psi}{\partial y\partial t}+\frac{\partial\psi}{\partial y}\frac{\partial^2\psi}{\partial x\partial y}-\frac{\partial\psi}{\partial x}\frac{\partial^2\psi}{\partial y^2}=\frac{\partial}{\partial y}\left[\left|\frac{\partial^2\psi}{\partial y^2}\right|^{n-1}\frac{\partial^2\psi}{\partial y^2}\right]+RiT+RiNC, \tag{7}$$

$$\frac{\partial T}{\partial t}+\frac{\partial\psi}{\partial y}\frac{\partial T}{\partial x}-\frac{\partial\psi}{\partial x}\frac{\partial T}{\partial y}=\frac{1}{Pr}\frac{\partial}{\partial y}\left[\left|\frac{\partial^2\psi}{\partial y^2}\right|^{n-1}\frac{\partial T}{\partial y}\right], \tag{8}$$

$$Sc\left[\frac{\partial C}{\partial t}+\frac{\partial\psi}{\partial y}\frac{\partial C}{\partial x}-\frac{\partial\psi}{\partial x}\frac{\partial C}{\partial y}\right]=\frac{\partial^2 C}{\partial y^2}. \tag{9}$$

The boundary conditions (5) now become

$$\begin{aligned}&\frac{\partial\psi}{\partial x}=\frac{\partial\psi}{\partial y}=0,\ T=\frac{x}{t^2},\ C=\frac{x}{t^2}\ \text{at}\ y=0,\\&\frac{\partial\psi}{\partial y}\to 0,\ T\to 0,\ C\to 0\ \text{as}\ y\to\infty.\end{aligned} \tag{10}$$

Here $Pr = K/\rho\alpha$ is the Prandtl number, $Sc=\frac{DRe_n^{\frac{1}{(n+1)}}}{UL}$ is the Schmidt number, $Ri = Gr/Re^2 = 1$ is the Richardson number, $Gr = \rho^2 g\beta_T(T_w - T_\infty)L^3/K^2$ is the Grashof number, $N = \beta_C(C_w - C_\infty)/\beta_T(T_w - T_\infty)$ is the buoyancy ratio parameters.

3. Lie group of transformations

It is known that similarity solution is important in many fields in sciences and engineering. It is necessary to seek a general approach to apply it to those novel problems. The Lie group transformation technique is a well-developed theory about continuous symmetry of mathematical objects and structures and can be used for many subjects of contemporary mathematics and modern theoretical physics. It is expected that this theory can provide us with a new methodology for analyzing the continuous symmetries of governing equations of heat fluid flows in non-Newtonian fluids. It reduces the number of independent variables of the partial differential equations under consideration and keeps the system and associated initial and boundary condition invariant. It should be noted that several researchers have made attempts to incorporate the Lie group transformation technique. Examples include Asghar et al. [41], and Uddin et al. [42]. Reviews for the fundamental theory and applications of Lie group analysis to differential equations may be found in the texts by Olver [43], Bluman and Kumei [44], Cantwell [45]. We select following two parameters linear group of transformations (a special form of Lie group transformation)

$$\begin{aligned}&x^*=tA^{\alpha_1},\ x^*=xB^{\beta_1},\ \psi^*=\psi A^{\alpha_2}B^{\beta_2},\\&y^*=yA^{\alpha_3}B^{\beta_3},\ T^*=TA^{\alpha_4}B^{\beta_4},\ C^*=CA^{\alpha_5}B^{\beta_5},\end{aligned} \tag{11}$$

where A, B, α_i, $\beta_i (i = 1, 2, \ldots, 5)$ are constants. We seek the values of α_i, β_i such that the form of Eqs. (7)–(9) is invariant under the transformations. Eqs. (7)–(9) will be invariant if α_i, β_i, are connected by

$$\begin{aligned}&\alpha_2=\frac{1-2n}{(1+n)}\alpha_1,\alpha_3=\frac{2-n}{(1+n)}\alpha_1,\alpha_4=-2\alpha_1,\alpha_5=-2\alpha_1,\\&\beta_2=\frac{2n}{(1+n)}\beta_1,\beta_3=\frac{n-1}{(1+n)}\beta_1,\beta_4=\beta_1,\beta_5=\beta_1.\end{aligned} \tag{12}$$

With these relationship of α_i, β_i, Eq. (11) becomes

$$\begin{aligned}&x^*=tA^{\alpha_1},\ x^*=xB^{\beta_1},\ \psi^*=\psi A^{\left(\frac{1-2n}{1+n}\right)\alpha_1}B^{\left(\frac{2n}{1+n}\right)\beta_1},\\&y^*=yA^{\left(\frac{2-n}{1+n}\right)\alpha_1}B^{\left(\frac{n-1}{1+n}\right)\beta_1},T^*=TA^{-2\alpha_1}B^{\beta_1},\ C^*=CA^{-2\alpha_1}B^{\beta_1}.\end{aligned} \tag{13}$$

Next, we seek "absolute invariants" under this group of transformations, i.e., functions having the same form before and after the transformation.

3.1. Similarity transformations (absolute invariants)

It is seen from Eqs. (11) and (13) that

$$\frac{y^*}{t^{*\left(\frac{2-n}{1+n}\right)}x^{*\left(\frac{n-1}{1+n}\right)}}=\frac{y}{t^{\left(\frac{2-n}{1+n}\right)}x^{\left(\frac{n-1}{1+n}\right)}}. \tag{14}$$

This combination is therefore absolute invariant, and we denote this invariant by

$$\eta=\frac{y}{t^{\left(\frac{2-n}{1+n}\right)}x^{\left(\frac{n-1}{1+n}\right)}}. \tag{15}$$

By the same argument, other absolute invariants are

$$f(\eta)=\frac{\psi}{t^{\left(\frac{2n-1}{1+n}\right)}x^{\left(\frac{2n}{1+n}\right)}},\ \theta(\eta)=\frac{t^2}{x}T,\ \phi(\eta)=\frac{t^2}{x}C. \tag{16}$$

3.2. Similarity differential equations

Using the similarity transformations in Eqs. (15) and (16) into Eqs. (7)–(9), we obtain the following similarity equations,

$$n|f''|^{n-1}f'''+f'+\left(\frac{2-n}{n+1}\right)\eta f''-f'^2+\left(\frac{2n}{n+1}\right)ff''+\theta+N\phi=0, \tag{17}$$

$$\frac{1}{Pr}\left[(n-1)|f''|^{n-2}f'''\theta'+|f''|^{n-1}\theta''\right]+2\theta+\left(\frac{2-n}{n+1}\right)\eta\theta'-f'\theta+\left(\frac{2n}{n+1}\right)f\theta'=0, \tag{18}$$

$$\frac{1}{Sc}\phi''+2\phi+\left(\frac{2-n}{n+1}\right)\eta\phi'-f'\phi+\left(\frac{2n}{n+1}\right)f\phi'=0. \tag{19}$$

The transformed boundary conditions are

$$f(0)=f'(0)=0,\ \theta(0)=\phi(0)=1,\ f'(\infty)=\theta(\infty)=\phi(\infty)=0. \tag{20}$$

Here primes denote derivatives with respect to the similarity independent variable η.

3.3. Validity of our group analysis

It is interesting to note that for $n = 1$, we can recover the similarity solutions reported by Kolomenskiy and Mofatt [46] and Bachok et al. [47] which confirm our two parameters group method. In the absence of the heat and mass transfer, it is worth mentioning that Eq. (17) for $n = 1$ becomes identical with Eq. (6) found by Fang et al. [48] for the unsteady two-dimensional shrinking sheet when $\beta = 1$

4. Physical quantities

The quantities of interest are the skin friction factor $C_{f\bar{x}}$, the local Nusselt number $Nu_{\bar{x}}$ and the local Sherwood number $Sh_{\bar{x}}$ can be found from the following definition:

$$C_{f\bar{x}} = \frac{2\tau_w}{\rho U^2},\ Nu_{\bar{x}} = \frac{\bar{x}q_w}{k(T_w - T_\infty)},\ Sh_{\bar{x}} = \frac{\bar{x}J_w}{D(C_w - C_\infty)}, \tag{21}$$

where τ_w, q_w, J_w are shear stress, the wall heat flux and the wall mass flux (dimensional) and are defined as

$$\tau_w = \mu\left(\frac{\partial\bar{u}}{\partial\bar{y}}\right)^n_{\bar{y}=0},\ q_w = -k\left(\frac{\partial\bar{u}}{\partial\bar{y}}\right)^{n-1}_{\bar{y}=0}\left(\frac{\partial T}{\partial\bar{y}}\right)_{\bar{y}=0},\ J_w = -D\left(\frac{\partial C}{\partial\bar{y}}\right)_{\bar{y}=0}. \tag{22}$$

Using variables (6), (15), (16) and (22), we can show that normalized $C_{f\bar{x}}, Nu_{\bar{x}}$ and $Sh_{\bar{x}}$ are proportional $|f''(0)|^n$, $-\theta'(0)$ and $-\phi'(0)$.

5. Results and discussion

The transformation of the governing equations reduces the numerical work significantly. The resulting system of coupled equations and associated boundary conditions is solved by the Runge–Kutta–Fehlberg fourth-fifth order numerical method with shooting technique [49]. Graphical representation of results is very useful to discuss the physical features presented by the solutions. This section describes the influence of some interesting parameters on the dimensionless velocity, temperature and concentration fields. The influences of the entering parameters on the dimensionless velocity, temperature and concentration are shown in Figs. 2–13.

5.1. Velocity profiles

The behavior of velocity when the foreign mass within the boundary layer is Hydrogen (Sc = 0.22 approx.), water vapor (Sc = 0.60 approx.) and methanol (Sc = 1.0) at approximately 25 °C and 1 atm is shown in Fig. 2 when $Ri = n = N = 1$ and Pr = 6.2 (air). Schmidt number is the ratio of viscous diffusion to molecular (species) diffusion. For $Sc < 1$, molecular diffusion rate exceeds the momentum diffusion rate and vice versa for $Sc > 1$. Sub-unity values of Schmidt number will therefore result in a deceleration in the flow (reduced skin friction), which will also decrease thermal diffusion rates. Conversely mass transfer will be accentuated in the regime with increasing Sc values. This can be observed in Table 1. The parameter $n = 1$ stands for Newtonian fluid and the buoyancy parameter $N = 1$ stands for buoyancy aiding flow where thermal buoyancy and concentration buoyancy are of comparable order. It is found that in the vicinity of the plate, the velocity of the methanol is higher than that of Hydrogen. However, the velocity of the water vapor is lower than that of methanol of Hydrogen gas. The boundary layer thickness of water vapor is higher than that of methanol and Hydrogen. This figure also shows the effects of the similarity variable $\eta(x, y, t)$ on the velocity. It is found that the nondimensional velocity enhances as nondimensional time progresses from the beginning to the steady-state condition. Fig. 3 shows the dimensionless velocity profiles in the boundary layer for different values of the Prandtl number Pr when $Ri = n = N = 1$ and Sc = 1.0. Pr is the ratio of momentum diffusivity to thermal diffusivity for a given nanofluid. With lower Pr fluids, heat diffuses faster than momentum (the energy diffusion rate exceeds the viscous diffusion rate) and vice versa for higher Pr fluids. With an increase in Pr, velocity will rise when Pr changes from 1 to 6.2. Reverse trends of velocity are noticed when Pr changes from 0.2 to 1. The buoyancy ratio $N = \beta_C(C_w - C_\infty)/\beta_T(T_f - T_\infty)$ represents the relative magnitude of species buoyancy and thermal buoyancy forces. For $N = 1$ these two forces are of the same magnitude. For $N > 0$, species buoyancy is dominant and opposite for $N < 1$. The weaker contribution of thermal buoyancy force for $N < 1$ results in a depletion in local Nusselt number. The stronger contribution of species buoyancy force for $N > 1$ induces enhancement in the local Sherwood number. The momentum field is coupled to the concentration (species) field via the linear species buoyancy force, $N\phi$, in the momentum Eq. (17). Effect of the buoyancy ratio N on the dimensionless velocity profiles is investigated in Fig. 4 for constant values $Ri = n = Sc$ = 1.0 and Pr = 6.2. As expected when the buoyancy ratio increases boundary layer thickness increases. In this state for N = 0.0 firstly boundary layer grows on the opposite side and then returns to regular side. Fig. 5 presents the

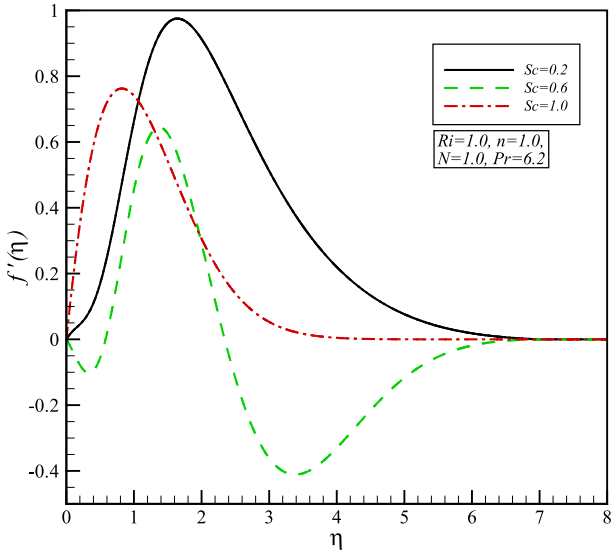

Figure 2 Effect of the Schmidt number Sc on the dimensionless velocity profile.

Table 1 Values of skin friction factor, Nusselt number and Sherwood number for different values of the parameters Sc, Pr, N and n.

Sc	Ri	Pr	N	n	$C_{f\bar{x}}$	$Nu_{\bar{x}}$	$Sh_{\bar{x}}$
1	1	6.2	1	1	2.08464	3.75463	3.17568
0.6	1	6.2	1	1	−1.27488	−4.87027	4.01747
0.2	1	6.2	1	1	1.02746	−4.23367	1.94564
1	1	0.2	1	1	2.90657	0.85986	0.02343
1	1	1	1	1	2.25657	1.87947	2.56748
1	1	6.2	0	1	−1.94098	−3.98048	−7.49086
1	1	6.2	2	1	2.37469	2.59017	1.84765
1	1	6.2	1	2	2.08464	3.75463	3.17568

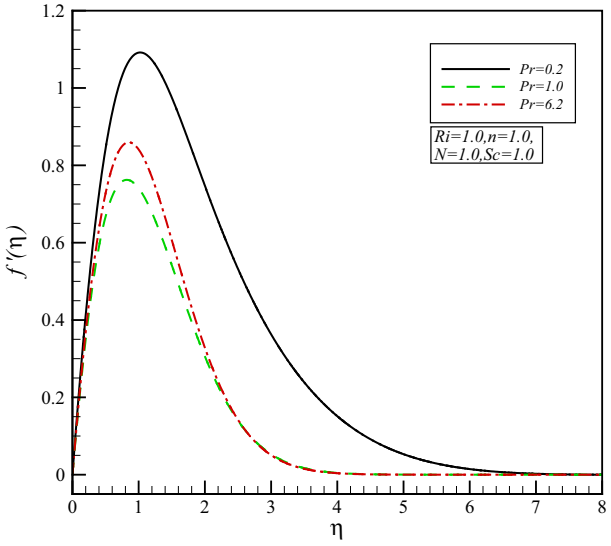

Figure 3 Effect of the Prandtl number *Pr* on the dimensionless velocity profile.

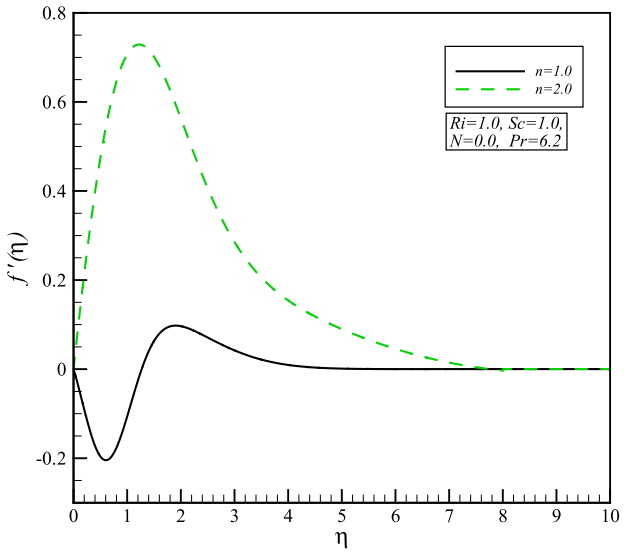

Figure 5 Effect of the power law *n* on the dimensionless velocity profile.

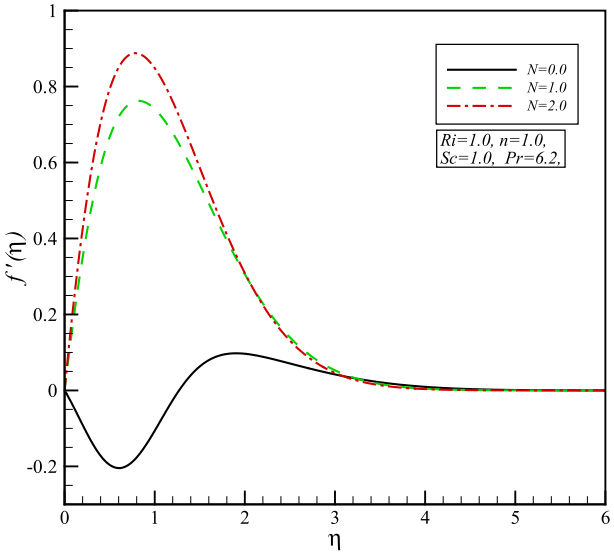

Figure 4 Effect of the buoyancy ratio *N* on the dimensionless velocity profile.

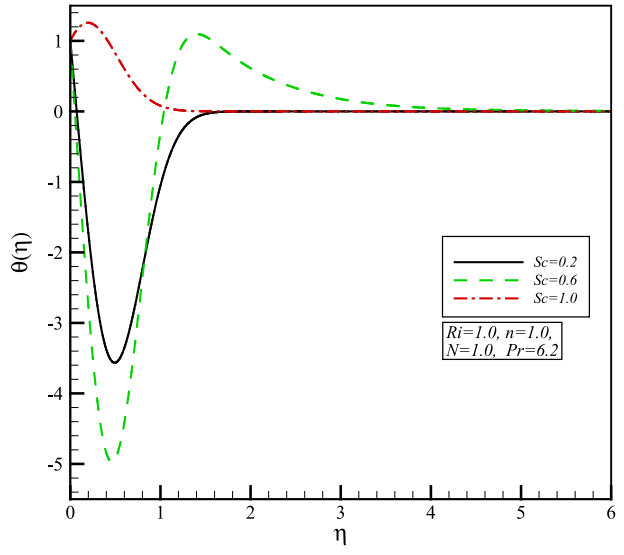

Figure 6 Effect of the Schmidt number *Sc* on the dimensionless temperature profile.

variations of the velocity boundary layer for the different values of power flow n when $Ri = Sc = 1.0$, and $Pr = 6.2$. It is clear that for $n = 2$ boundary layer thickness is much larger. In addition, for $n = 1$ firstly boundary layer grows on the opposite side and then returns to regular side.

5.2. Temperature profiles

Fig. 6 shows the dimensionless temperature distributions in the thermal boundary layer for different values of the Schmidt number when $Ri = n = N = 1.0$ and $Pr = 6.2$. As Sc increases, the thermal boundary layer thickness increases firstly and then decreases but this trend is also associated with side changes. It is noteworthy that for $Sc = 1.0$ the temperature gradient at the edge of vertical plate is positive and for $Sc = 0.2, 0.6$ this amount is negative. This figure also shows the effects of the similarity variable $\eta(x, y, t)$ on the temperature. It is found that as the non-dimensional temperature enhances as non-dimensional time progresses from the beginning to the steady-state condition. Effect of the Prandtl number on the thermal boundary-layer when $Ri = n = N = 1.0$ and $Sc = 1.0$ is shown in Fig. 7. It is clear that as the Prandtl number increases, the thickness of the thermal boundary-layer decreases as the curves become increasingly steeper. This is in agreement with the physical fact that the thermal boundary-layer thickness decreases with increasing Prandtl number. Fig. 8 illustrates the effect of the buoyancy ratio N on the temperature profile for constant values $Ri = n = Sc = 1.0$ and $Pr = 6.2$. As expected when the buoyancy ratio increases thermal boundary layer thickness decreases, but for $N = 0.0$

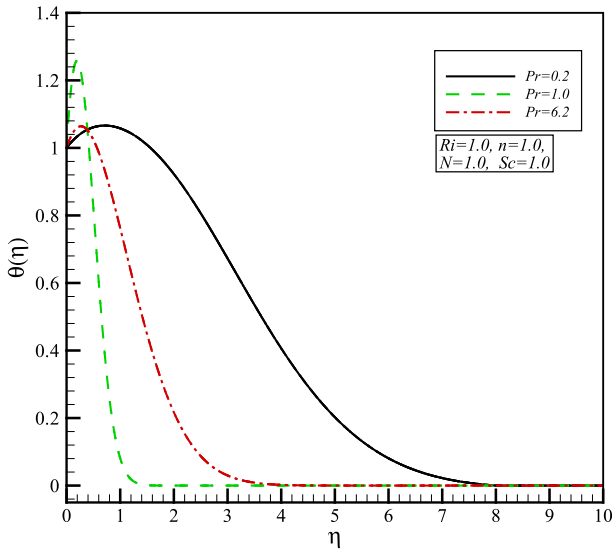

Figure 7 Effect of the Prandtl number *Pr* on the dimensionless temperature profile.

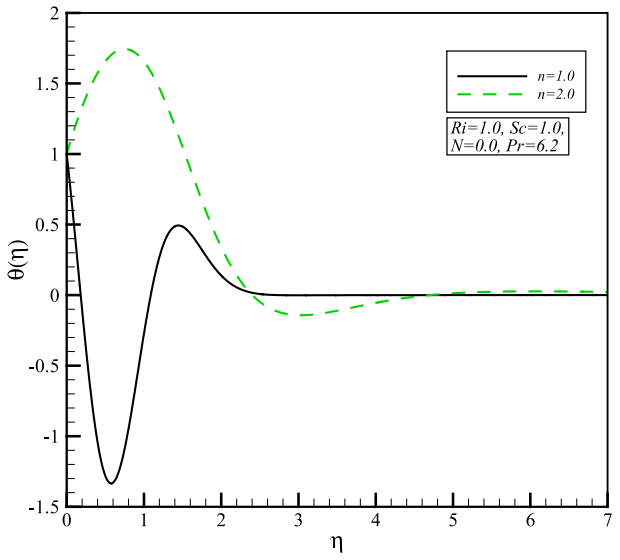

Figure 9 Effect of the power law *n* on the dimensionless temperature profile.

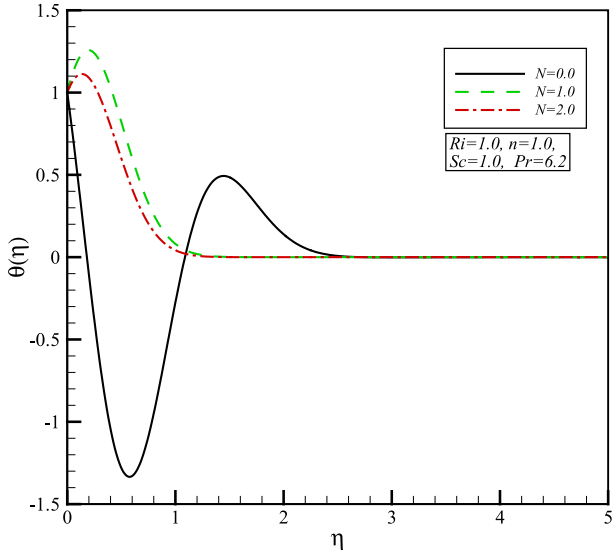

Figure 8 Effect of the buoyancy ratio *N* on the dimensionless temperature profile.

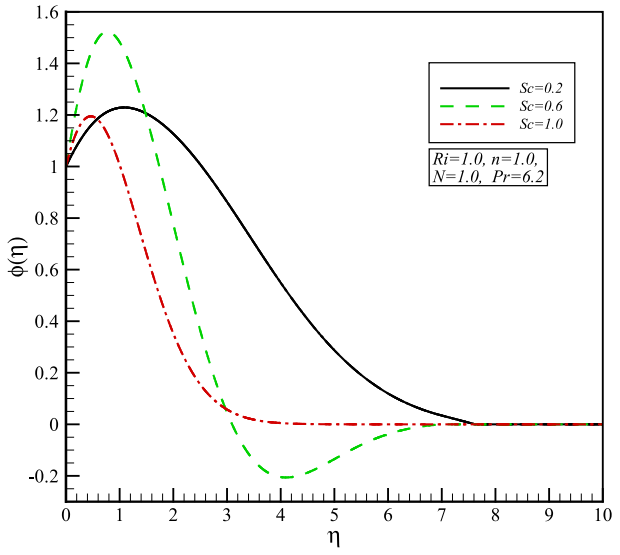

Figure 10 Effect of the Schmidt number *Sc* on the dimensionless concentration profile.

firstly boundary-layer grows on the opposite side and then returns to regular side. The temperature profiles are depicted in Fig. 9 for different values of power law *n* and fix parameters $Ri = Sc = 1.0$, $N = 0.0$, and $Pr = 6.2$. It is clear that for $n = 2$ thermal boundary-layer thickness is much larger. In addition, for $n = 1$ firstly boundary-layer grows on the opposite side and then returns to regular side. Temperature increases as the index n increases.

5.3. Concentration profiles

Fig. 10 reveals variation of the dimensionless concentration graph in response to a change in Schmidt number when $Ri = n = N = 1.0$ and $Pr = 6.2$. The influence of Schmidt number on the dimensionless concentration profile graph is as the values of Schmidt number increase, the curves of concentration boundary-layer become increasingly steeper. But variation of concentration boundary layer thickness with indeterminate is indeterminate. Fig. 11 shows that as the Prandtl number decreases, the species concentration drops more rapidly as the thickness of the concentration boundary-layer decreases. Resent results are obtained for $Ri = n = N = 1.0$ as fix values. For constant values $Ri = n = N = 1.0$ and $Pr = 6.2$. It was observed in Fig. 12 that as the buoyancy ratio increases, the concentration boundary-layer decreases. It is highlighted that for $N = 0.0$ manner of graph is different. In this statue concentration gradient at the edge of vertical plate is negative; therefore, concentration boundary-layer grows on the opposite side and then returns to positive position. It should be mentioned that boundary-layer thickness at negative

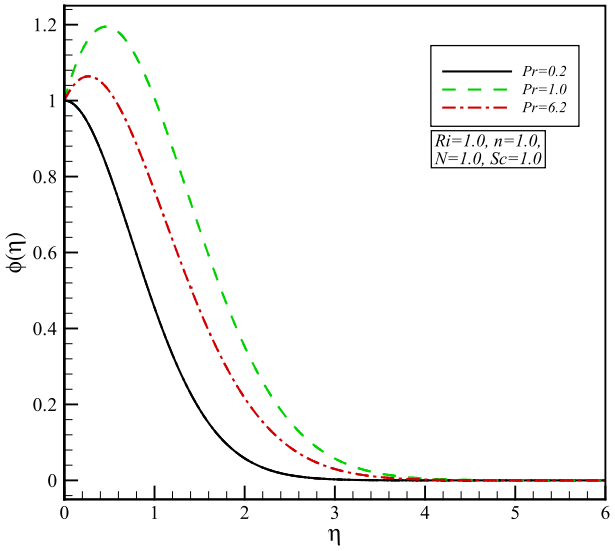

Figure 11 Effect of the Prandtl number Pr on the dimensionless concentration profile.

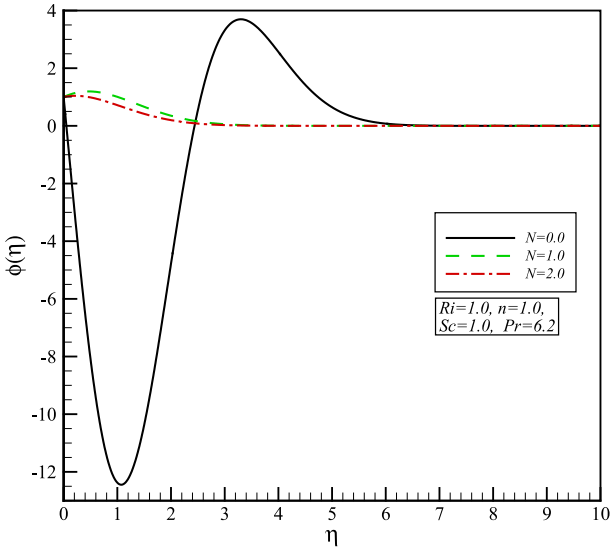

Figure 12 Effect of the buoyancy ratio N on the dimensionless concentration profile.

side is rather than positive side. Finally in Fig. 13 the concentration profiles are depicted for different values of power flow n and fix parameters $Ri = Sc = 1.0$, $N = 0.0$ and $Pr = 6.2$. Similar to velocity and temperature profiles, trend of concentration profiles is different for $n = 1.0$ and $n = 2.0$. Boundary-layer thickness for $n = 2.0$ is thinner rather than $n = 1.0$ but for recent case concentration gradient at the edge of vertical plate is negative; therefore, concentration boundary layer grows on the opposite side and then returns to positive position.

Also, for investigation of the parameters of physical interest, Table 1 is presented. In this table numerical values of the skin friction factor, Nusselt number and Sherwood number for different values of the parameters Sc, Pr, N and n are included. The mentioned notification of Figs. 2–16 can be

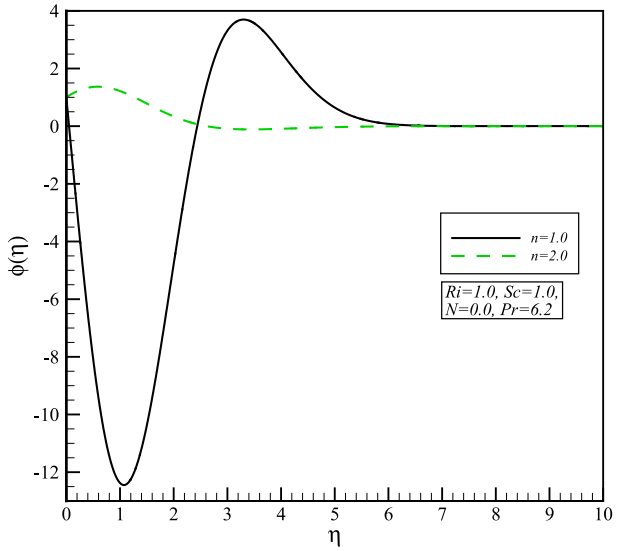

Figure 13 Effect of the power law n on the dimensionless concentration profile.

observed in Table 1. Particularly, it should be highlighted that sign of the skin friction factor $C_{f\bar{x}}$, the local Nusselt number $Nu_{\bar{x}}$ and the local Sherwood number $Sh_{\bar{x}}$ (slope of velocity, temperature and concentration profiles, respectively) can be changed by variations of Sc, Ri and N. Also it is observed that in contrast to changing the parameters there is not a regular manner for physical quantities, generally. Because of unavailability of theoretical or experimental data for the problem of unsteady non-Newtonian free convection (power-law fluids), it is not possible to compare our results. Therefore, there is a need for more systematic studies to compare and evaluate the flow and the heat/mass transfer situations.

6. Conclusions

A mathematical model for the unsteady flow of a non-Newtonian fluid adjacent to a vertical plate has been developed. The governing partial differential equations for mass, momentum, energy and concentration have been reduced to a triplet of coupled, nonlinear ordinary differential equations as well as relevant boundary conditions via the single applications of two parameters Lie group transformation method. These equations are solved by a numerical method (fourth-order Runge–Kutta scheme with the shooting method). The novel aspect of this paper can be extracted as follows:

(i) Friction factor and heat transfer for methanol are higher than those of hydrogen and water vapor, and reversed trend is noticed for mass transfer rate.
(ii) Friction factor decreases while heat and mass transfer rates increase as the Prandtl number increases.
(iii) Friction factor increases while heat and mass transfer rates decrease as the buoyancy ration increases.
(iv) Friction factor increases while heat and mass transfer rates decrease as the buoyancy ration increases.
(v) Friction (heat and mass transfer rate) factor of Newtonian fluid is higher (lower) than the dilatant fluid.

The present study has been restricted to regular fluid flows. Future investigations will consider non-Newtonian nanofluids and will be communicated shortly.

References

[1] M.M. Rashidi, S.A. Mohimanian pour, S. Abbasbandy, Analytic approximate solutions for heat transfer of a micropolar fluid through a porous medium with radiation, Commun. Nonlinear Sci. Numer. Simul. 16 (2011) 1874–1889.

[2] M. Sajid, T. Hayat, S. Asghar, Comparison between the HAM and HPM solutions of thin film flows of non-Newtonian fluids on a moving belt, Nonlinear Dynam. 50 (2007) 27–35.

[3] M.J. Uddin, N.H.Md. Yusoff, O. Anwar Bég, A.I.Md. Ismail, Lie group analysis and numerical solutions of boundary layer flow of non-Newtonian nanofluids along a horizontal plate in porous medium with internal heat generation, Phys. Scr. 87 (2013) 025401.

[4] O.D. Makinde, Thermal stability of a reactive third grade fluid in a cylindrical pipe: an exploitation of Hermite-Pade approximation technique, Appl. Math. Comput. 189 (2007) 690–697.

[5] O.D. Makinde, Hermite-Pade approximation approach to thermal criticality for a reactive third-grade liquid in a channel with isothermal walls, Int. Commun. Heat Mass Transfer 34 (7) (2007) 870–877.

[6] J.B.R. Loureiroa, A.P. Silva Freirea, Asymptotic analysis of turbulent boundary-layer flow of purely viscous non-Newtonian fluids, J. Non-Newtonian Fluid Mech. 199 (2013) 20–28.

[7] G. Davaa, T. Shigechi, S. Momoki, Effects of viscous dissipation on fully developed heat transfer of non-Newtonian fluids in plane laminar Poiseuille-Couette flow, Int. Commun. Heat Mass Transfer 31 (5) (2004) 663–672.

[8] M. El-Shahed, MHD of a fractional viscoelastic fluid in a circular tube, Mech. Res. Commun. 33 (2006) 261–268.

[9] M. Firouzi, S.H. Hashemabadi, Analytical solution for Newtonian-Bingham plastic two-phase pressure driven stratified flow through the circular ducts, Int. Commun. Heat Mass Transfer 35 (5) (2008) 666–673.

[10] T. Hayat, R. Ellahi, S. Asghar, The influence of variable viscosity and viscous dissipation on the non-Newtonian flow: an analytical solution, Commun. Nonlinear Sci. Numer. Simul. 12 (2007) 300–313.

[11] O. Jambal, T. Shigechi, G. Davaa, S. Momoki, Effects of viscous dissipation and fluid axial heat conduction on heat transfer for non-Newtonian fluids in ducts with uniform wall temperature. Part I: parallel plates and circular ducts,, Int. Commun. Heat Mass Transfer 32 (9) (2005) 1165–1173.

[12] M. Sajid, T. Hayat, S. Asghar, On the analytic solution of the steady flow of a fourth grade fluid, Phys. Lett. A 355 (2006) 18–26.

[13] Tasawar Hayat, Anum Shafiq, Ahmed Alsaedi, Effect of joule heating and thermal radiation in flow of third grade fluid over radiative surface, PLoS ONE (2014).

[14] A. Shafiq, M. Nawaz, T. Hayat, A. Alsaedi, Magnetohydrodynamic axisymmetric flow of a third grade fluid between two porous disks, Braz. J. Chem. Eng. 30 (3) (2013).

[15] R. Dhanai, P. Rana, L. Kumar, Critical values in slip flow and heat transfer analysis of non-Newtonian nanofluid utilizing heat source/sink and variable magnetic field: multiple solutions, J. Taiwan Inst. Chem. Eng. 58 (2016) 155–164.

[16] A. Pantokratoras, Non-similar Blasius and Sakiadis flow of a non-Newtonian Carreau fluid, J. Taiwan Inst. Chem. Eng. 56 (2015) 1–5.

[17] M. Shojaeian, M. Yildiz, A. Koşar, Convective heat transfer and second law analysis of non-Newtonian fluid flows with variable thermophysical properties in circular channels, Int. Commun. Heat Mass Transfer 60 (2015) 21–31.

[18] X. Sia, X. Zhua, L. Zhenga, X. Zhangc, P. Lin, Laminar film condensation of pseudo-plastic non-Newtonian fluid with variable thermal conductivity on an isothermal vertical plate, Int. J. Heat Mass Transf. 92 (2016) 979–986.

[19] A.M. Megahed, Flow and heat transfer of a non-Newtonian power-law fluid over a non-linearly stretching vertical surface with heat flux and thermal radiation, Meccanica 50 (2015) 1693–1700.

[20] T. Sarpkaya, Flow of non-Newtonian fluids in a magnetic field, AIChE. J. 7 (1961) 324–328.

[21] D.S. Djukic, On the use of Crocco's equation for the flow of power-law fluids in a transverse magnetic field, AIChE J. 19 (1973) 1159–1163.

[22] D.S. Djukic, Hiemenz magnetic flow of power-law fluids, J. Appl. Mech. 41 (1974) 822–823.

[23] H.I. Andersson, K.H. Bach, B.S. Dandapat, Magnetohydrodynamic flow of a power-law flow over a stretching sheet, Int. J. Non-Linear Mech. 27 (1992) 929–936.

[24] M. Kumari, G. Nath, MHD boundary layer flow of a non-Newtonian fluid over a continuously moving surface with a parallel free stream, Acta Mech. 146 (2001) 139–150.

[25] S.J. Liao, On the analytic solution of magnetohydrodynamic flows of non-Newtonian fluids over a stretching sheet, J. Fluid Mech. 488 (2003) 189–212.

[26] R.B. Bird, Useful non-Newtonian models, Ann. Rev. Fluid Mech. 8 (1976) 13–34.

[27] C. Ming, L. Zheng, X. Zhang, Steady flow and heat transfer of the power-law fluid over a rotating disk, Int. Commun. Heat Mass Transfer 38 (2011) 280–284.

[28] J.P. Pascal, Similarity solutions for axisymmetric plane radial power law fluid flows through a porous medium, Comput. Math. Appl. 23 (1992) 25–41.

[29] J.P. Pascal, H. Pascal, Non-linear effects on some unsteady non-Darcian flows through porous media, Int. J. Non-Linear Mech. 32 (1997) 361–376.

[30] T.Ch. Wen, T. Hsiao, Unsteady forced convection heat transfer on a flat plate embedded in the fluid-saturated porous medium with inertia effect and thermal dispersion, Int. J. Heat Mass Transf. 45 (2002) 1563–1569.

[31] C.I. Cookey, A. Ogulu, V.B. Omubo-Pepple, Influence of viscous dissipation and radiation on unsteady MHD free-convection flow past an infinite heated vertical plate in a porous medium with time-dependent suction, Int. J. Heat Mass Transf. 46 (2003) 2305–2311.

[32] K.S. Chiem, Y. Zhao, Numerical study of steady/unsteady flow and heat transfer in porous media using a characteristics-based matrix-free implicit FV method on unstructured grids, Int. J. Heat Fluid Flow 25 (2004) 1015–1033.

[33] J.K. Lee, R.S.R. Gorla, I. Pop, Natural convection to power-law fluids from a heated vertical plate in a stratified environment, Int. J. Heat Fluid Flow 13 (1992) 259–265.

[34] A. Hossain, S. Bhowmick, R.S.R. Gorla, Unsteady mixed-convection boundary layer flow along a symmetric wedge with variable surface temperature, Int. J. Eng. Sci. 44 (2006) 607–620.

[35] M.C. Ece, E. Buyuk, Similarity solutions for free convection to power-law fluids from a heated vertical plate, Appl. Math. Lett. 15 (2002) 1–5.

[36] N.S. Elgazery, Transient analysis of heat and mass transfer by natural convection in power-law fluid past a vertical plate immersed in a porous medium (numerical study), Appl. Appl. Math. 3 (6) (2008) 267–285.

[37] J.H. Merkin, I. Pop, Mixed convection along a vertical surface: similarity solutions for uniform flow, Fluid Dyn. Res. 30 (2002) 233–250.

[38] M.M. Rashidi, T. Hayat, M. Keimanesh, A.A. Hendi, New analytical method for the study of natural convection flow of a

non-Newtonian, Int. J. Numer. Meth. Heat Fluid Flow 23 (3) (2013) 436–450.
[39] M.M. Rashidi, O. Anwar Bég, M.T. Rastegari, A study of non-Newtonian flow and heat transfer over a non-isothermal wedge using the homotopy analysis method, Chem. Eng. Commun. 199 (2) (2012) 231–256.
[40] N. Galanis, M.M. Rashidi, Entropy generation in non-Newtonian fluids due to heat and mass transfer in the entrance region of ducts, Heat Mass Transf. 48 (9) (2012) 1647–1662.
[41] S. Asghar, M. Jalil, M. Hussan, M. Turkyilmazoglu, Lie group analysis of flow and heat transfer over a stretching rotating disk, Int. J. Heat Mass Transf. 69 (2014) 140–146.
[42] M.J. Uddin, O.A. Bég, N. Amin, Hydromagnetic transport phenomena from a stretching or shrinking nonlinear nanomaterial sheet with Navier slip and convective heating: a model for bio-nano-materials processing, J. Magn. Magn. Mater. 2014 (38) (2014) 252–261.
[43] P.J. Olver, Application of Lie Groups to Differential Equations, Springer, New York, NY, USA, 1989.
[44] G.M. Bluman, S. Kumei, Symmetries and Differential Equations, Springer-Verlag, 1989.
[45] B.J. Cantwell, Introduction to Symmetry Analysis, Cambridge University Press, 2003.
[46] D. Kolomenskiy, H.K. Mofatt, Similarity solutions for unsteady stagnation point flow, J. Fluid Mech. 711 (2012) 394–410.
[47] N. Bachok, A. Ishak, I. Pop, Unsteady boundary-layer flow and heat transfer of a nanofluid over a permeable stretching/shrinking sheet, Int. J. Heat Mass Transf. 55 (7) (2012) 2102–2109.
[48] T. Fang, J. Zhang, S.-S. Yao, Viscous flow over an unsteady shrinking sheet with mass transfer, Chin. Phys. Lett. 26 (2009) 014703.
[49] F.M. White, Viscous Fluid Flow, second ed., McGraw-Hill, New York, 1991.
[50] M.M. Rashidi, E. Erfani, Analytical method for solving steady MHD convective and slip flow due to a rotating disk with viscous dissipation and ohmic heating, Eng. Comput. 29 (6) (2012) 562–579.
[51] M.M. Rashidi, M. Ali, N. Freidoonimehr, B. Rostami, M. Anwar Hossain, Mixed convective heat transfer for MHD viscoelastic fluid flow over a porous wedge with thermal radiation, Adv. Mech. Eng. 2014 (2014) 735939.
[52] M.M. Rashidi, E. Momoniat, M. Ferdows, A. Basiriparsa, Lie group solution for free convective flow of a nanofluid past a chemically reacting horizontal plate in a porous media, Math. Probl. Eng. (2014) 239082.
[53] F. Garoosi, L. Jahanshaloo, M.M. Rashidi, A. Badakhsh, M.A. Ali, Numerical simulation of natural convection of the nanofluid in heat exchangers using a Buongiorno model, Appl. Math. Comput. 254 (2015) 183–203.
[54] N. Freidoonimehr, M.M. Rashidi, S. Mahmud, Unsteady MHD free convective flow past a permeable stretching vertical surface in a nano-fluid, Int. J. Therm. Sci. 87 (2015) 136–145.